Available online at www.sciencedirect.com
ScienceDirect
Franklin Institute 00 (2022) 1–16
Franklin Institute

Linear Quadratic Integral Differential Game applied to the Real-time Control of a Quadrotor Experimental setup

Hadi Nobahari, Ali BaniAsad, Reza Pordal, Alireza Sharifi

Abstract

The accurate attitude control of a quadrotor is necessary, especially when facing disturbance. Moreover, all the flight states of the quadrotor are not measured in practice. In this study, a linear quadratic Gaussian with integral action based on the differential game theory is implemented on the quadrotor experimental setup. A continuous state-space model of the setup is derived using the linearization of nonlinear equations of motion, and its parameters are identified with the experimental results. Next, the attitude control commands of the quadrotor are derived based on two players; one finds the best attitude control command, and the other creates the disturbance by mini-maximizing a quadratic criterion, defined as the sum of outputs plus the weighted control effort and disturbance. The performance of the proposed structure is investigated in level flight and compared to the linear quadratic regulator controller. Results demonstrate that the proposed approach has an excellent performance in dissipating the disturbances.

Keywords:
Linear Quadratic Gaussian, Differential Game, Quadrotor, State Estimation, 3DoF Experimental setup, Optimal Control, Robust Control.

1. Introduction

A quadrotor is a type of helicopter with four rotors that plays a significant role in today's society [1], including research, military, imaging, recreation, and agriculture. The performance of the quadrotor relies on the control system, including attitude, altitude, and position subsystems. In the attitude control of the quadrotor, it is vital to maintain the attitude outputs at the desired level using control commands, such as the rotational speed of the rotors [2], when disturbances occur suddenly. Therefore, much research is being conducted on the automatic control of the attitudes' quadrotor in facing the disturbance. In [3, 4], a Proportional Integral Derivative (PID) controller is used to regulate the quadrotor attitude. However, the control objectives have not been effectively achieved with this controller when the disturbance occurs. To solve this problem, the model-based approaches [5, 6] are utilized for controller design. These controllers work based on information from the quadrotor's attitude model and disturbance to produce the best control command.

Various model-based controllers can be found within the literature, the most well-known of which are intelligent control, the nonlinear control, robust control, and optimal control to reduce the disturbance effect in the attitude control and provide a faster control algorithm in facing the modeling error. In the intelligent controller category,

Email addresses: nobahari@sharif.edu (Hadi Nobahari), ali.baniasad@ae.sharif.edu (Ali BaniAsad), email address (Reza Pordal), alireza_sharifi@ae.sharif.edu (Alireza Sharifi)

the artificial intelligence computing approaches like fuzzy logic [7] iterative learning [8] machine learning [9], reinforcement learning [10], and evolutionary computation [11] have been utilized to regulate the quadrotor's attitude. Nonlinear control methods such as Feedback Linearization (FBL) [12], Sliding Mode Control (SMC) [13] and Synergetic Control [14] have been applied to control the roll, pitch, and yaw angles of the quadrotor. Moreover, robust control strategies such as H_∞ [15, 16] and μ-synthesis [17] have been implemented to stabilize the quadrotor attitudes based on the worst-case scenario and large uncertainty ranges. In the optimal controller category, a Linear Quadratic Regulator (LQR) [18] and Linear Quadratic Gaussian (LQG) [19] have been im-plemented on the quadrotor based on the minimization of a quadratic criterion, including regulation performance and control effort to provide optimally controlled feedback gains. Linear Quadratic Regulator Differential Game (LQR-DG) control approach [20, 21] is a class of optimal and robust controller methods that controls the outputs of a system based on its linear model and mini-maximization of a cost function. This approach has been utilized to stabilize and control various nonlinear and complex systems such as a ship controller [22, 23]. Moreover, in the LQR-DG control method, the control commands are analytically generated based on a pursuit-evasion of two players, one tracks the best control command, and the other creates the disturbance. This is one of the distinctive features of the LQR-DG controller and an important difference from other optimal control methods.

In this study, a LQG controller method based on the differential game theory, with an integral action called Linear Quadratic Integral Gaussian Differential Game (LQIG-DG) controller, is proposed to generate the most efficient control command for an experimental setup of the quadrotor when facing the disturbance. Since the LQIG-DG is affected by an accurate model of the system, first, the dynamic of the three-degree-of-freedom setup of the quadrotor is modeled. Then, the linear state-space form the quadrotor model is extracted using the linearization of the nonlinear equations of motion to utilize in the proposed control problem. Moreover, the model's parameters are identified and verified against the experimental values. Next, the flight states of the quadrotor setup are estimated based on an Extended Kalman Filter (EKF) [24, 25] and then compensated using the LQIG-DG controller architecture. Finally, the LQIG-DG technique is applied to the experimental setup of the quadrotor to reduce the effect of disturbance. The performance of the suggested controller is examined when the disturbance occurs. The results show the successful performance of the LQIR-DG scheme in reducing the disturbance.

In the remainder of this study, the problem is defined in section 2. In sections 3, the dynamics model for the experimental setup of the quadrotor and the estimation problem are derived in details, respectively. In section 4, the LQIR-DG architecture is denoted. Finally, in sections 5 and 6, numerical results and conclusion are provided, respectively.

2. Problem Statement

Here, a nonlinear dynamic is presented for the setup of the quadrotor, as illustrated in figure 1. The quadrotor is free to rotate about its roll, pitch, and yaw axes. The acceleration and the angular velocities along three orthogonal axes are measured using the low-cost Inertial Measurement Unit (IMU). These noisy measurements are utilized in a nonlinear filter for the estimation of the quadrotor states, including the Euler angles and angular velocities. These estimated states are compensated in the structure of the LQIG-DG controller to stabilize the quadrotor setup. The block diagram of the controller structure is illustrated in Fig. 2.

3. Modeling of the Quadrotor Setup

Here, the model of the three-degree-of-freedom setup of the quadrotor is presented in detail. For this purpose, first, the configuration of the quadrotor is denoted. Then, the nonlinear model of the attitude dynamics is derived from denoting the state-space form. Finally, the nonlinear model is linearized to utilize for control purposes.

3.1. Configuration of the Quadrotor

Figure 3 denotes the quadrotor schematic. Each rotor has an angular velocity, Ω_r, rotating about the z_B axis in the body coordinate system. Rotors 1 and 3 rotate counterclockwise, while rotors 2 and 4 rotate clockwise to cancel yawing moment.

Figure 1: 3DoF setup of the quadrotor.

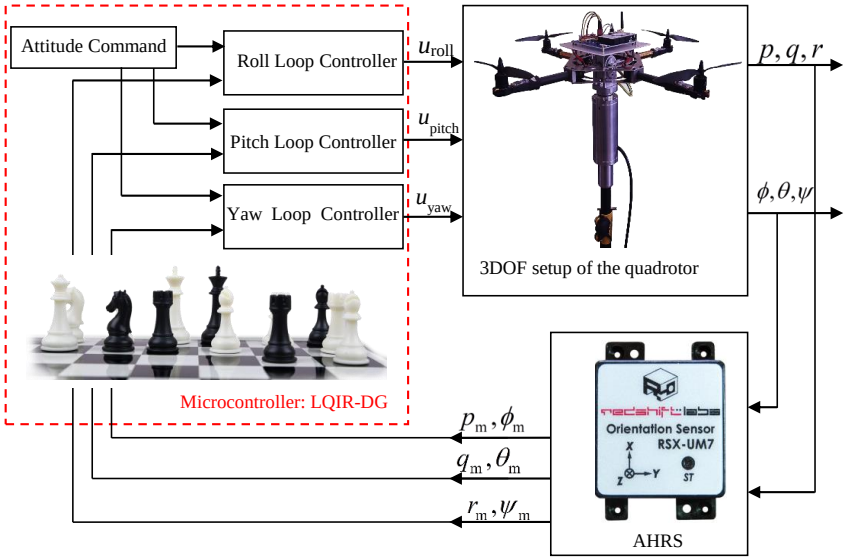

Figure 2: Block diagram of the LQIG-DG controller structure.

3.2. Dynamic Model

The quadrotor kinetic model, derived using the Newton-Euler method, is stated as [26, 27]

$$\dot{p} = \frac{I_{yy} - I_{zz}}{I_{xx}} qr + q\frac{I_{rotor}}{I_{xx}}\Omega_r + \frac{u_{roll}}{I_{xx}} + \frac{d_{roll}}{I_{xx}} \tag{1}$$

$$\dot{q} = \frac{I_{zz} - I_{xx}}{I_{yy}} rp + p\frac{I_{rotor}}{I_{xx}}\Omega_r + \frac{u_{pitch}}{I_{yy}} + \frac{d_{pitch}}{I_{yy}} \tag{2}$$

$$\dot{r} = \frac{I_{xx} - I_{yy}}{I_{zz}} pq + \frac{u_{yaw}}{I_{zz}} + \frac{d_{yaw}}{I_{zz}} \tag{3}$$

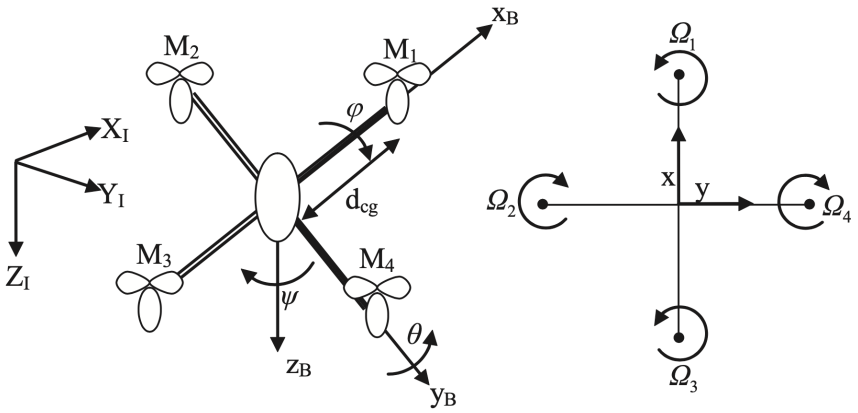

Figure 3: Configuration of the quadrotor.

where (p, q, r) are the angular velocities. d_{roll}, d_{pitch}, and d_{yaw} are the disturbances generated in x_B, y_B, and z_B, respectively. Moreover, I_{xx}, I_{yy}, and I_{zz} are the principal moment of inertia, and I_{rotor} is a rotor inertia about its axis. The relation between the angular body rates and the Euler angles rates are obtained as

$$\dot{\phi} = p + (q\sin(\phi) + r\cos(\phi))\tan(\theta) \tag{4}$$

$$\dot{\theta} = q\cos(\phi) - r\sin(\phi) \tag{5}$$

$$\dot{\psi} = (q\sin(\phi) + r\cos(\phi))/\cos(\theta) \tag{6}$$

where (ϕ, θ, ψ) are roll, pitch, and yaw angles. Moreover, Ω_r, called the overall residual rotor angular velocity, is computed as

$$\Omega_r = -\Omega_1 + \Omega_2 - \Omega_3 + \Omega_4 \tag{7}$$

3.3. Control Commands

The control inputs u_{roll}, u_{pitch}, and u_{yaw} are roll, pitch, and yaw moments, obtained from the rotors, defined as

$$u_{\text{roll}} = \text{b}\,\text{d}_{\text{cg}}(\Omega_2^2 - \Omega_4^2) \tag{8}$$

$$u_{\text{pitch}} = \text{b}\,\text{d}_{\text{cg}}(\Omega_1^2 - \Omega_3^2) \tag{9}$$

$$u_{\text{yaw}} = \text{d}(\Omega_1^2 - \Omega_2^2 + \Omega_3^2 - \Omega_4^2) \tag{10}$$

Also, d and b are, respectively, drag and thrust coefficients. d_{cg} is the distance of rotors from the gravity center. Hence, the angular velocity commands are obtained as

$$\Omega_{c,1}^2 = \Omega_{\text{mean}}^2 + \frac{1}{2\text{b}\,\text{d}_{\text{cg}}}u_{\text{pitch}} + \frac{1}{4d}u_{\text{yaw}} \tag{11}$$

$$\Omega_{c,2}^2 = \Omega_{\text{mean}}^2 + \frac{1}{2\text{b}\,\text{d}_{\text{cg}}}u_{\text{roll}} - \frac{1}{4d}u_{\text{yaw}} \tag{12}$$

$$\Omega_{c,3}^2 = \Omega_{\text{mean}}^2 - \frac{1}{2\text{b}\,\text{d}_{\text{cg}}}u_{\text{pitch}} + \frac{1}{4d}u_{\text{yaw}} \tag{13}$$

$$\Omega_{c,4}^2 = \Omega_{\text{mean}}^2 - \frac{1}{2\text{b}\,\text{d}_{\text{cg}}}u_{\text{roll}} - \frac{1}{4d}u_{\text{yaw}} \tag{14}$$

where Ω_{mean} is the nominal of the rotor angular velocities.

3.4. State-Space Form

Here, the state-space model is presented for control purposes. By defining $x_1 = p$, $x_2 = q$, $x_3 = r$, $x_4 = \phi$, $x_5 = \theta$, and $x_6 = \psi$; the model of in state-space form are denoted as

$$\dot{x}_1 = \frac{\mathrm{I_{yy}} - \mathrm{I_{zz}}}{\mathrm{I_{xx}}} x_2 x_3 + x_2 \frac{\mathrm{I_{rotor}}}{\mathrm{I_{xx}}} \Omega_r + \frac{u_{\mathrm{roll}}}{\mathrm{I_{xx}}} + \frac{d_{\mathrm{roll}}}{\mathrm{I_{xx}}} \tag{15}$$

$$\dot{x}_2 = \frac{\mathrm{I_{zz}} - \mathrm{I_{xx}}}{\mathrm{I_{yy}}} x_1 x_3 - x_1 \frac{\mathrm{I_{rotor}}}{\mathrm{I_{xx}}} \Omega_r + \frac{u_{\mathrm{pitch}}}{\mathrm{I_{yy}}} + \frac{d_{\mathrm{pitch}}}{\mathrm{I_{yy}}} \tag{16}$$

$$\dot{x}_3 = \frac{\mathrm{I_{xx}} - \mathrm{I_{yy}}}{\mathrm{I_{zz}}} x_1 x_2 + \frac{u_{\mathrm{yaw}}}{\mathrm{I_{zz}}} + \frac{d_{\mathrm{yaw}}}{\mathrm{I_{zz}}} \tag{17}$$

$$\dot{x}_4 = x_1 + (x_2 \sin(x_4) + x_3 \cos(x_4)) \tan(x_5) \tag{18}$$

$$\dot{x}_5 = x_2 \cos(x_4) - x_3 \sin(x_4) \tag{19}$$

$$\dot{x}_6 = (x_2 \sin(x_4) + x_3 \cos(x_4)) / \cos(x_5) \tag{20}$$

Equations (15)-(17) are rewritten in the following form:

$$\dot{x}_1 = \alpha_1 x_2 x_3 + \alpha_2 x_2 \Omega_r + \alpha_3 u_{\mathrm{roll}} + \alpha_3 d_{\mathrm{roll}} \tag{21}$$

$$\dot{x}_2 = \beta_1 x_1 x_3 - \beta_2 x_1 \Omega_r + \beta_3 u_{\mathrm{pitch}} + \beta_3 d_{\mathrm{pitch}} \tag{22}$$

$$\dot{x}_3 = \gamma_1 x_1 x_2 + \gamma_2 u_{\mathrm{yaw}} + \gamma_2 d_{\mathrm{yaw}} \tag{23}$$

The measurement model is written as

$$\mathbf{z} = \begin{bmatrix} p_m & q_m & r_m & \phi_m & \theta_m & \psi_m \end{bmatrix}^{\mathrm{T}} \tag{24}$$

3.5. Linear Model

The continuous-time linear model is utilized to drive the control commands on the quadrotor. The linear state-space model is denoted as

$$\dot{\mathbf{x}}(t) = \mathbf{A}\mathbf{x}(t) + \mathbf{B}\mathbf{u}(t) + \mathbf{B_d}\mathbf{d}(t) \tag{25}$$

where $\mathbf{A}$, $\mathbf{B}$, and $\mathbf{B_d}$ are the system, input and disturbance matrices, respectively. Moreover, $\mathbf{d}$ is the disturbance. The measurements equation is stated as

$$\mathbf{z}(t) = \mathbf{x}(t) \tag{26}$$

According to equations(15)-(20), the linear dynamic model around the equilibrium points ($\mathbf{x}_e = 0$ and $\mathbf{u}_e = 0$) of the quadrotor setup is denoted as

$$\begin{aligned} \dot{\mathbf{x}} = \begin{bmatrix} \dot{\mathbf{x}}_{\mathrm{roll}} \\ \dot{\mathbf{x}}_{\mathrm{pitch}} \\ \dot{\mathbf{x}}_{\mathrm{yaw}} \end{bmatrix} &= \begin{bmatrix} \mathbf{A}_{\mathrm{roll}} & \mathbf{0} & \mathbf{0} \\ \mathbf{0} & \mathbf{A}_{\mathrm{pitch}} & \mathbf{0} \\ \mathbf{0} & \mathbf{0} & \mathbf{A}_{\mathrm{yaw}} \end{bmatrix} \begin{bmatrix} \mathbf{x}_{\mathrm{roll}} \\ \mathbf{x}_{\mathrm{pitch}} \\ \mathbf{x}_{\mathrm{yaw}} \end{bmatrix} \\ &+ \begin{bmatrix} \mathbf{B}_{\mathrm{roll}} & \mathbf{0} & \mathbf{0} \\ \mathbf{0} & \mathbf{B}_{\mathrm{pitch}} & \mathbf{0} \\ \mathbf{0} & \mathbf{0} & \mathbf{B}_{\mathrm{yaw}} \end{bmatrix} \begin{bmatrix} \mathbf{u}_{\mathrm{roll}} \\ \mathbf{u}_{\mathrm{pitch}} \\ \mathbf{u}_{\mathrm{yaw}} \end{bmatrix} \\ &+ \begin{bmatrix} \mathbf{B}_{\mathrm{roll}} & \mathbf{0} & \mathbf{0} \\ \mathbf{0} & \mathbf{B}_{\mathrm{pitch}} & \mathbf{0} \\ \mathbf{0} & \mathbf{0} & \mathbf{B}_{\mathrm{yaw}} \end{bmatrix} \begin{bmatrix} \mathbf{d}_{\mathrm{roll}} \\ \mathbf{d}_{\mathrm{pitch}} \\ \mathbf{d}_{\mathrm{yaw}} \end{bmatrix} \end{aligned} \tag{27}$$

where $\mathbf{x}_{\mathrm{roll}} = \begin{bmatrix} p & \phi \end{bmatrix}^{\mathrm{T}}$, $\mathbf{x}_{\mathrm{pitch}} = \begin{bmatrix} q & \theta \end{bmatrix}^{\mathrm{T}}$, and $\mathbf{x}_{\mathrm{yaw}} = \begin{bmatrix} r & \psi \end{bmatrix}^{\mathrm{T}}$.

Moreover, the state and input matrices are presented as

$$\mathbf{A}_{\text{roll}} = \mathbf{A}_{\text{pitch}} = \mathbf{A}_{\text{yaw}} = \begin{bmatrix} 0 & 0 \\ 1 & 0 \end{bmatrix} \tag{28}$$

$$\mathbf{B}_{\text{roll}} = \begin{bmatrix} \frac{1}{\mathrm{I}_{\text{xx}}} \\ 0 \end{bmatrix};\ \mathbf{B}_{\text{pitch}} = \begin{bmatrix} \frac{1}{\mathrm{I}_{\text{yy}}} \\ 0 \end{bmatrix};\ \mathbf{B}_{\text{yaw}} = \begin{bmatrix} \frac{1}{\mathrm{I}_{\text{zz}}} \\ 0 \end{bmatrix} \tag{29}$$

3.6. System Identification

Here, the system identification was made using the simulation of the roll, pitch, and yaw states and sensor data output from the quadrotor setup. For this purpose, the same input is given to the simulated model and setup. In the case of system identification, the cost function was defined as the sum square error between simulations and quadrotor setup measurements. Then, the Nonlinear Least Squares (NLS) optimization technique minimizes the cost function. In NLS, the goal is to look for the model parameters vector $\rho = \begin{bmatrix} \alpha_1 & \alpha_2 & \alpha_3 & \beta_1 & \beta_2 & \beta_3 & \gamma_1 & \gamma_2 \end{bmatrix}$, which would minimize the sum of squares of residual errors. In other words, the following cost function has to minimize:

$$\text{Residual sum of squares} = RSS = \sum_{i=1}^{n} (y_i - \hat{y}_i)^2 \tag{30}$$

where y is the value of the variable to be predicted, and $\hat{y}$ is the predicted value of y, which $\hat{y}$ is a function of the 3DoF setup model parameters vector, ρ, and the system states, $\mathbf{x}$, i.e.:

$$\hat{y}_i = f(\mathbf{x}_i, \rho) \tag{31}$$

One way to minimize RSS is to differentiate RSS with respect to ρ, then set the differentiation to zero and solve for ρ, i.e.:

$$\frac{\partial}{\partial \rho_j} RSS = 0, \quad \forall j \in [1, n] \tag{32}$$

Since there is no closed-form solution for this system of equations, so iterative optimization technique has to be used in which, at each iteration k, minor adjustments have been made to the values of ρ as shown below, and re-evaluate RSS:

$$\rho_j^{(k)} = \rho_j^{(k-1)} + \delta\rho_j \tag{33}$$

Trust Region Reflective (TRR) has been devised to update ρ efficiently. To increase the accuracy of system identification, at first, the parameters of each channel were estimated separately, and then the coupled parameters of the attitude channels were modified. In the parameter modification process, after each parameter modification step mentioned above, the estimated parameters of the previous step are assumed to be fixed, and other parameters are modified. To identification of each stage, several experiments with different scenarios have been performed.

4. Formulation of the Controller Design

In the LQIR-DG controller structure, an integral action is added to the LQR-DG controller to cancel the steady-state errors for reference tracking. For this purpose, first, the augmented state space of the linear quadrotor model is defined to utilize in the controller architecture. Then, the LQR-DG controller design procedure is presented to produce the best control commands for the experimental setup of the quadrotor.

4.1. Augmented State Space Formulation

To add the integral action to the controller structure, the augmented states are defined as follows:

$$\mathbf{x_{a_i}} = \begin{bmatrix} \mathbf{x_i} & \int \mathbf{x_i} \end{bmatrix}^{\mathrm{T}} \tag{34}$$

where i = roll, pitch, and yaw. Then, the quadrotor dynamics model, denoted by Eq.(25), is denoted in the augmented state-space model as

$$\dot{\mathbf{x}}_{\boldsymbol{a}}(t) = \mathbf{A_a}\mathbf{x_a}(t) + \mathbf{B_a}\mathbf{u}(t) + \mathbf{B_{d_a}}\mathbf{d}(t) \tag{35}$$

where matrices $\mathbf{A_a}$ and $\mathbf{B_a}$ are defined as follows:

$$\mathbf{A_a} = \begin{bmatrix} \mathbf{A} & \mathbf{0} \\ \mathbf{I} & \mathbf{0} \end{bmatrix} \tag{36}$$

$$\mathbf{B_a} = \mathbf{B_{d_a}} = \begin{bmatrix} \mathbf{B} \\ \mathbf{0} \end{bmatrix} \tag{37}$$

In the above equation $\mathbf{I}$ denotes the identity matrix.

4.2. LQIR-DG Controller Method

The LQIR-DG controller is an optimal and robust method based on the differential game theory. This controller consists of two essential players: one finds the best control command, and the other creates the worst disturbance. For this purpose, the first player tries to minimize a cost function, while the second is assumed to maximize it. Therefore, the quadratic cost function equation is denoted using min-max operators as follows:

$$\min_u \max_d J(\mathbf{x_{a_i}}, u_i, d_i) = J(\mathbf{x_{a_i}}, u_i^*, d_i^*) = \min_u \max_d \int_0^{\mathrm{t_f}} \left(\mathbf{x_{a_i}^T Q_i x_{a_i}} + u_i^{\mathrm{T}} R u_i - d_i^{\mathrm{T}} R_d d_i \right) \mathrm{d}t \tag{38}$$

where R and R_d are symmetric nonnegative definite matrices and $\mathbf{Q_i}$ is a symmetric positive definite matrix. Moreover, $\mathrm{t_f}$ is the final time. ??????????????????To solve this problem, connections between the general optimal problem and the LQIR problem are considered [20]. Consequently, the optimum control effort is computed for each control loop as follows:

$$u_i(t) = -\mathbf{K}_{\boldsymbol{i}}(t)\mathbf{x_{a_i}}(t) \tag{39}$$

$$d_i(t) = \mathbf{K_{d_i}}(t)\mathbf{x_{a_i}}(t) \tag{40}$$

where $\mathbf{K_i}$ and $\mathbf{K_{d_i}}$ are a time varying gain, given by

$$\mathbf{K_i} = R^{-1}\mathbf{B}_{a_i}^{\mathbf{T}}\mathbf{P}_{a_i}(t) \tag{41}$$

$$\mathbf{K_{d_i}} = R_d^{-1}\mathbf{B}_{a_{d_i}}^{\mathbf{T}}\mathbf{P}_{a_{d_i}}(t) \tag{42}$$

where $\mathbf{P}_{a_i}(t)$ and $\mathbf{P}_{a_{d_i}}(t)$ satisfy

$$\dot{\mathbf{P}}_{a_i}(t) = -\mathbf{A_a^T}\mathbf{P_{a_i}}(t) - \mathbf{P_{a_i}}(t)\mathbf{A_a} - \mathbf{Q_i} + \mathbf{P_{a_i}}(t)\mathbf{S_{a_i}}(t)\mathbf{P_{a_i}}(t) + \mathbf{P_{a_i}}(t)\mathbf{S_{a_{d_i}}}(t)\mathbf{P_{a_{d_i}}}(t) \tag{43}$$

$$\dot{\mathbf{P}}_{a_{d_i}}(t) = -\mathbf{A_a^T}\mathbf{P_{a_{d_i}}}(t) - \mathbf{P_{a_{d_i}}}(t)\mathbf{A_a} - \mathbf{Q_i} + \mathbf{P_{a_{d_i}}}(t)\mathbf{S_{a_{d_i}}}(t)\mathbf{P_{a_{d_i}}}(t) + \mathbf{P_{a_{d_i}}}(t)\mathbf{S_{a_i}}(t)\mathbf{P_{a_i}}(t) \tag{44}$$

where $\mathbf{S_{a_i}} = \mathbf{B_{a_i}}R^{-1}\mathbf{B}_{a_i}^{\mathbf{T}}$ and $\mathbf{S_{a_{d_i}}} = \mathbf{B}_{a_{d_i}}R_d^{-1}\mathbf{B}_{a_{d_i}}^{\mathbf{T}}$. In this study, the steady-state values of the above equations ($\mathbf{P}$ as $\mathrm{t_f} \rightarrow \infty$) are utilized to generate a feedback control law.

5. Result and Discussion

Here, the results of the LQIR-DG controller method are devoted to the control loops of the roll, pitch, and yaw of the experimental setup of the quadrotor. First, the controller parameters are tuned using the results of numerical simulations. Moreover, the performance of the LQIR-DG controller is compared to an LQR control strategy. The quadrotor parameters are shown in table 1. Moreover, the parameters of LQIR-DG controller weight are denoted in table 2.

Table 1: The Parameter of the Quadrotor

Parameter	***Value***	***Unit***
I_{xx}	0.02839	kg.m^2
I_{yy}	0.03066	kg.m^2
I_{zz}	0.0439	kg.m^2
I_{rotor}	4.4398×10^{-5}	kg.m^2
b	3.13×10^{-5}	N. sec^2 /rad^2
d	3.2×10^{-6}	N.m. sec^2 /rad^2
Ω_{mean}	3000	rpm
d_{cg}	0.2	m

Table 2: The Parameters of the LQIR-DG Controller

Control Loop	***Weight***	***Value***
Roll	$\mathbf{Q}_{roll}$	diag([0.02, 65.96, 83.04, 0.00])
Pitch	$\mathbf{Q}_{pitch}$	diag([435.01, 262.60, 262.60, 0.00])
Yaw	$\mathbf{Q}_{yaw}$	diag([$4e-4$, 0.00, 0.133, 0])
-	R	1
-	R_d	1.2764

5.1. Evaluation of the 3DoF experimental setup model

Here, the performance of the extracted model of the 3DoF experimental setup is evaluated under three scenarios: (i) each channel separately, (ii) coupling between roll and pitch channel, and (iii) coupling between roll, pitch, and yaw channel. In the first scenario, each channel's parameters are changed.

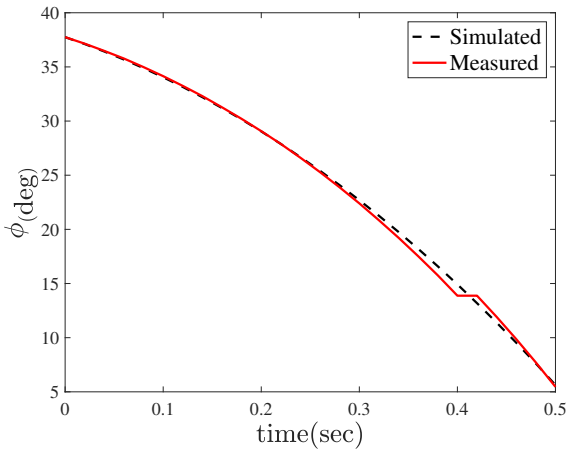

Figure 4: Comparison of roll channel states in simulation and 3DoF setup

Parameter	Value	Value after evaluation
α_3	1.1×10^{-4}	5.47×10^{-5}

Table 3: Comparison of roll channel parameter values before and after evaluation

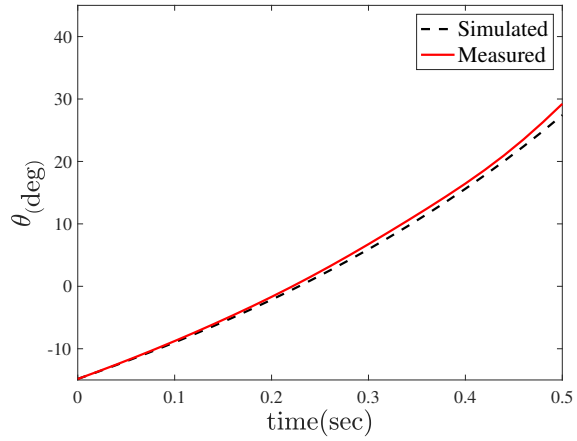

Figure 5: Comparison of pitch channel states in simulation and 3DoF setup

Parameter	Value	Value after evaluation
β_3	1.1×10^{-4}	7.13×10^{-5}

Table 4: Comparison of pitch channel parameter values before and after evaluation

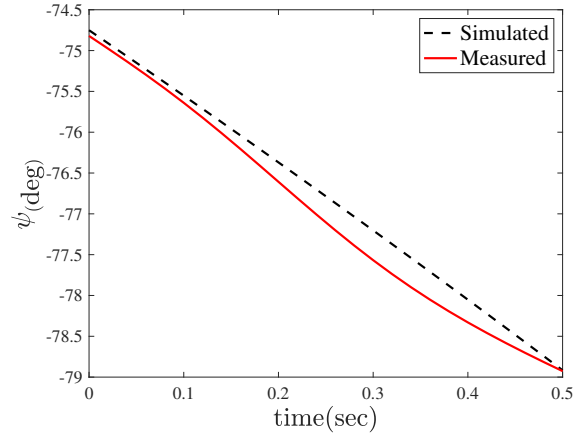

Figure 6: Comparison of yaw channel states in simulation and 3DoF setup

Parameter	Value	Value after evaluation
γ_2	5.5×10^{-5}	1.3×10^{-6}

Table 5: Comparison of yaw channel parameter values before and after evaluation

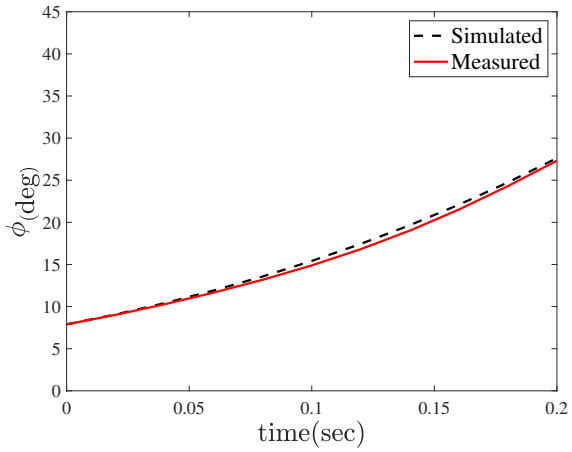

Figure 7: Comparison of roll channel states in simulation and 3DoF setup

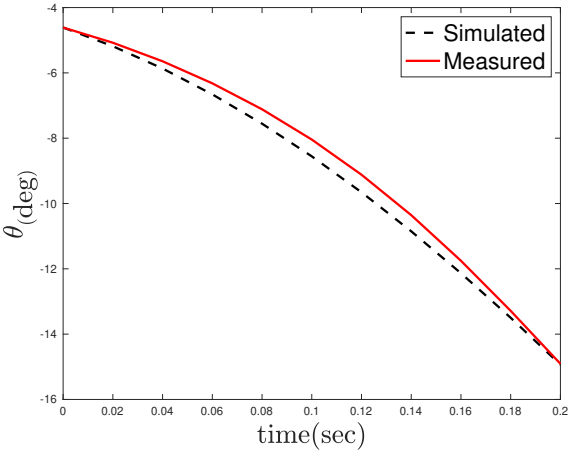

Figure 8: Comparison of pitch channel states in simulation and 3DoF setup

Parameter	Value	Value after evaluation
α_2	0.0015	0.0020
β_2	0.0015	0.0027

Table 6: Comparison of roll-pitch channel parameter values before and after evaluation

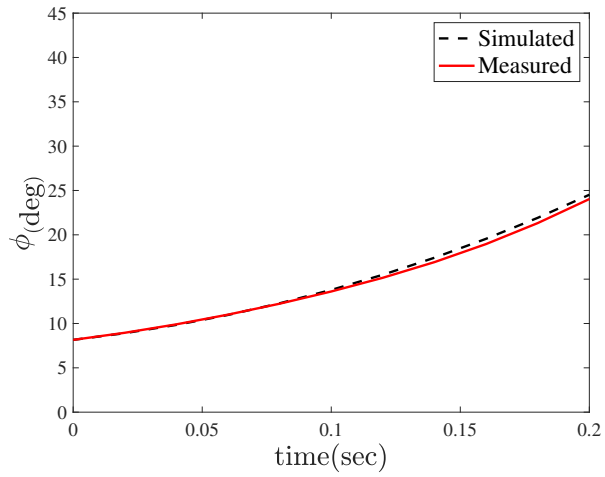

Figure 9: Comparison of roll channel states in simulation and 3DoF setup

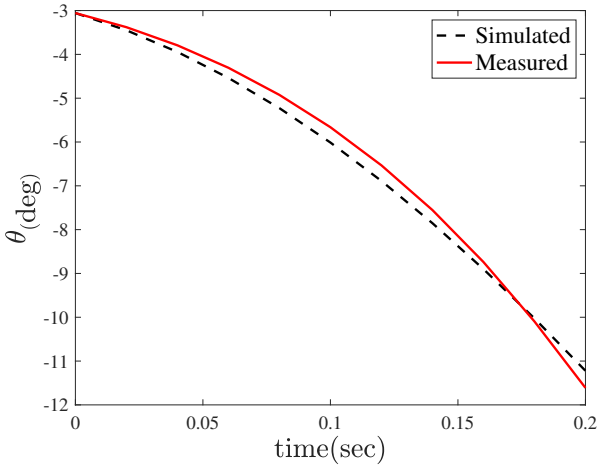

Figure 10: Comparison of pitch channel states in simulation and 3DoF setup

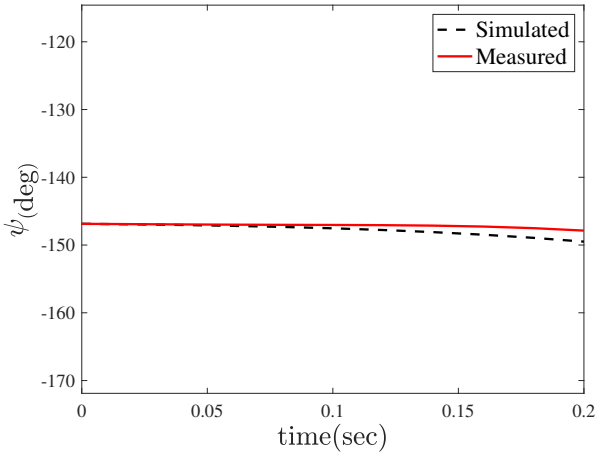

Figure 11: Comparison of yaw channel states in simulation and 3DoF setup

Parameter	Value	Value after evaluation
α_1	-0.9628	-1.56
β_1	0.9629	1.57
γ_1	-0.0017	-0.085

Table 7: Comparison of 3DOF channel parameter values before and after evaluation

5.2. Performance of the LQIR-DG Controller

Here, the performance of the LQIR-DG controller is evaluated. The desired and actual outputs, including the roll, pitch, and yaw angles, are compared in figure 12. The desired scenario of the simulator is considered a level flight. These figures show that the attitude outputs of the quadrotor converge to the desired values in less than three seconds. Moreover, figure 13 shows the angular velocity command of the quadrotor, respectively. These results illustrate that the LQIR-DG approach appropriately controls the attitude of the experimental setup of the quadrotor.

Figure 14 illustrates the performance of the LQIR-DG controller in the coupling mode of the roll and pitch channels to track the desired angle as a square wave with a frequency of 0.02 Hz and an amplitude of 20 degrees.

5.3. Investigating the possibility of disturbance rejection

This section investigates the possible rejection of input disturbances by the LQIR-DG controller in regulation. For this purpose, a disturbance with an amplitude of 0.5 N is added to the input from 20 to 60 seconds. As shown in figure 15, the LQIR-DG controller performs well in coupling the roll and screw channels to remove the input disturbance. 15 (a), the performance of this controller is checked by comparing the desired roll angle with the actual roll angle. Also, 15 (b) compares the desired pitch angle with the actual pitch angle of the 3DoF experimental setup in removing the input disturbance. The results indicate the proper performance of the controller in removing the input disturbance.

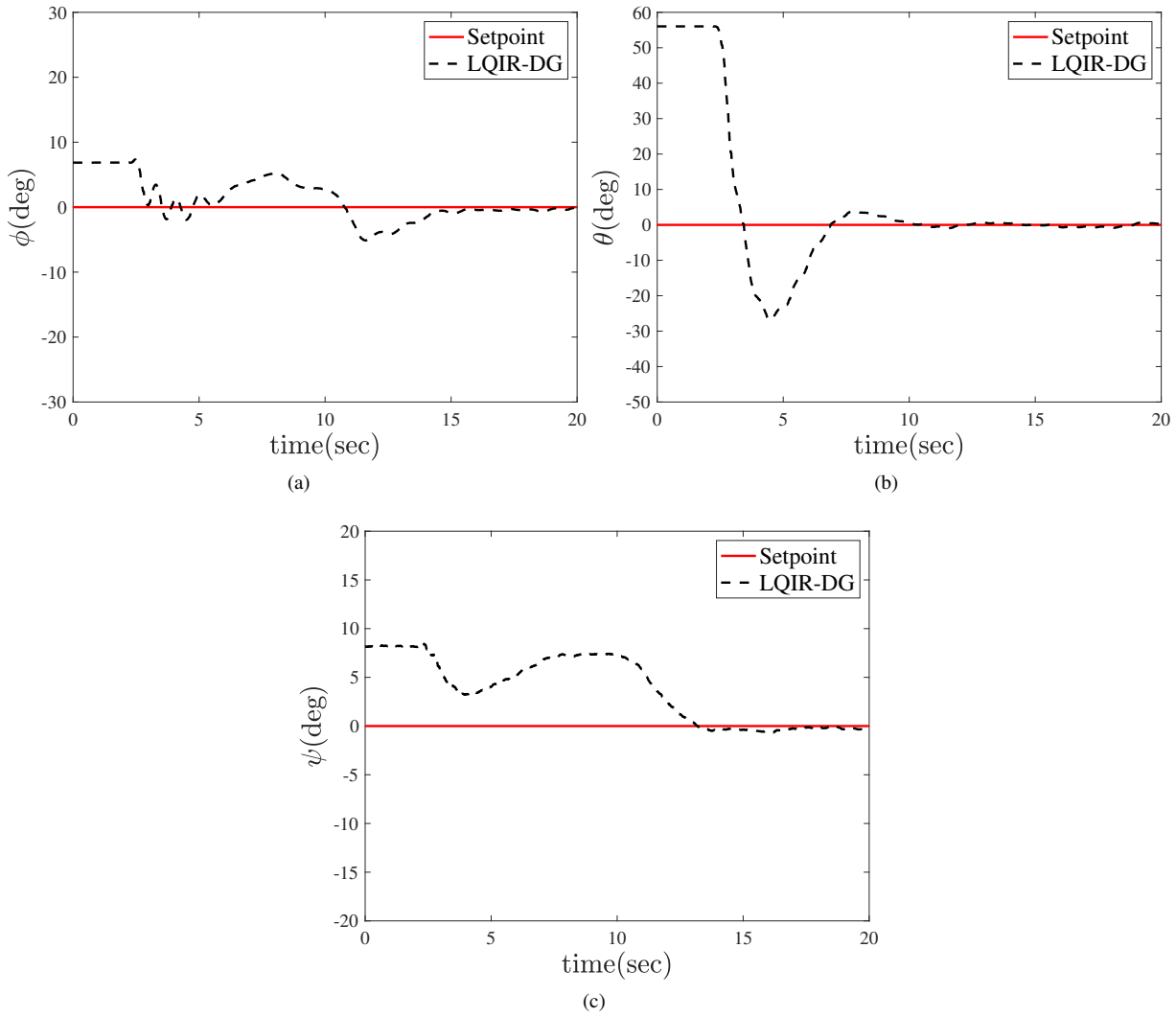

Figure 12: Performance of the LQIR-DG controller (a) roll angle (b) pitch angle (c) yaw angle

5.4. Investigating the impact of uncertainty in modeling

This section examines the performance of the LQIR-DG controller designed by considering the uncertainty in 3DoF experimental setup modeling. The performance of the sliding mode controller in the coupling mode of the roll, pitch, and yaw channels is checked by considering the uncertainty in the 3DoF experimental setup modeling in figure 16. For this purpose, 50 grams is added to the roll axis and 100 grams to the pitch axis. In figure 16 (a), the performance of this controller is checked by comparing the desired roll angle with the actual roll angle; In figure 16 (b), the performance of this controller is checked by comparing the desired pitch angle to the actual pitch angle. Also, figure 16 (c) compares the desired yaw angle with the actual yaw angle of the 3DoF experimental setup. The implementation results indicate the proper efficiency of the LQIR-DG controller in pursuit of the desired value, taking into account the uncertainty in the values of the moments of inertia around each axis of the body coordinate system.

5.5. Comparison with LQR

Here, the LQIR-DG controller performance is compared with famous control strategies such as the LQR controller method. Figure17 compares the quadrotor's desired and actual pitch angle in the presence of these controllers. This

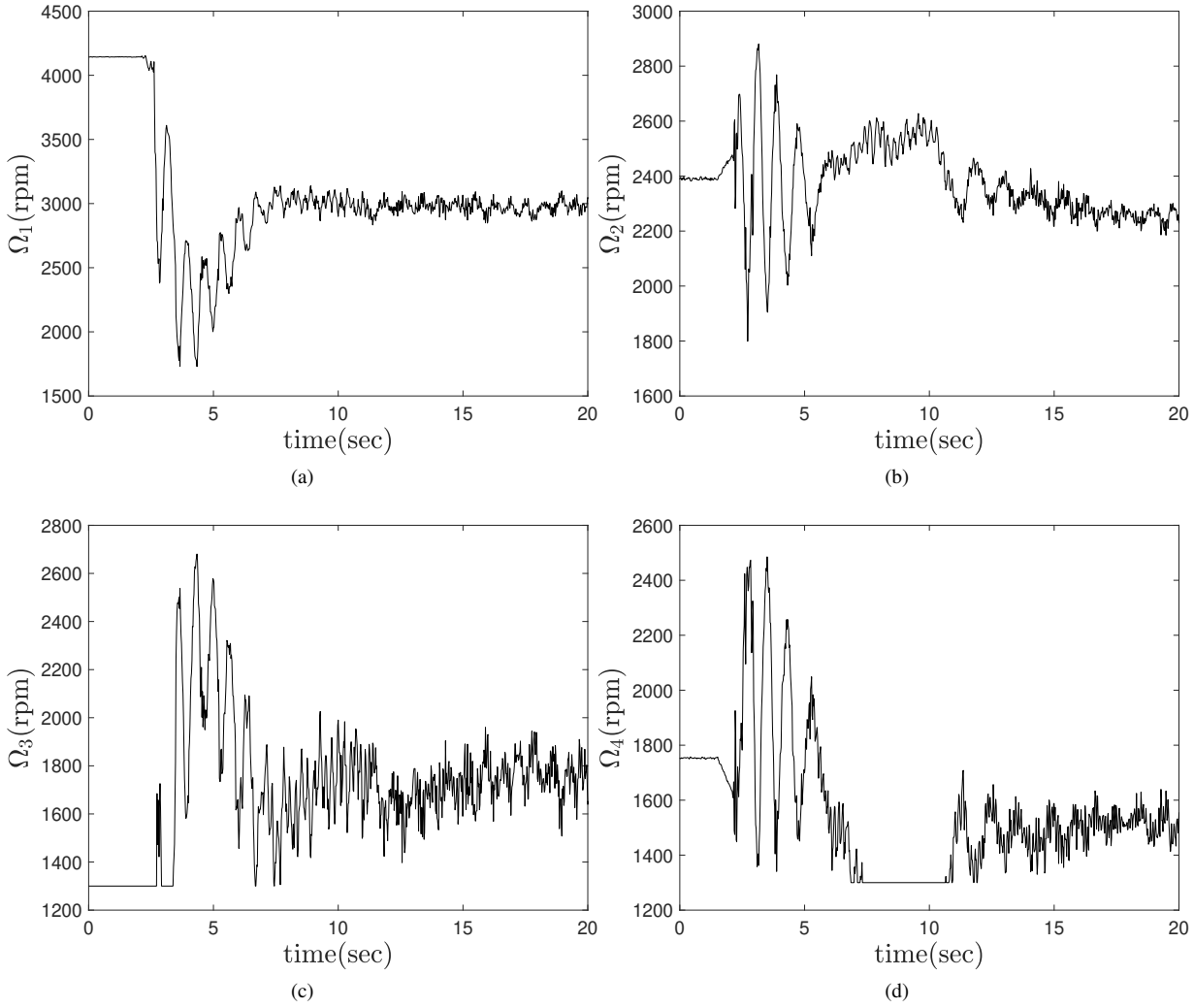

Figure 13: Time history of angular velocity commands

result indicates that the LQIR-DG controller can provide high tracking performance, such as good transient response and high rapid convergence relative to the LQR controller for pitch angle control of the quadrotor setup.

6. Conclusion

In this study, a linear quadratic with integral action based on the differential game theory, called LQIR-DG, was implemented for level attitude control in an experimental setup of a quadrotor. To implement the proposed controller structure, first, an accurate model of the quadrotor was linearized in the state-space form, and then the model parameters were estimated. Next, two players were considered for each of the quadrotor's roll, pitch, and yaw channels. The first player found the best control command for each channel of the setup of a quadrotor based on the mini-maximization of a quadratic criterion; when the second player produced the worst disturbances. Finally, the performance of the proposed controller was investigated in level flight and compared to the LQR controller. The implementation results verify the successful performance of the LQIR-DG method in the level flight of the attitude control for the actual plant.

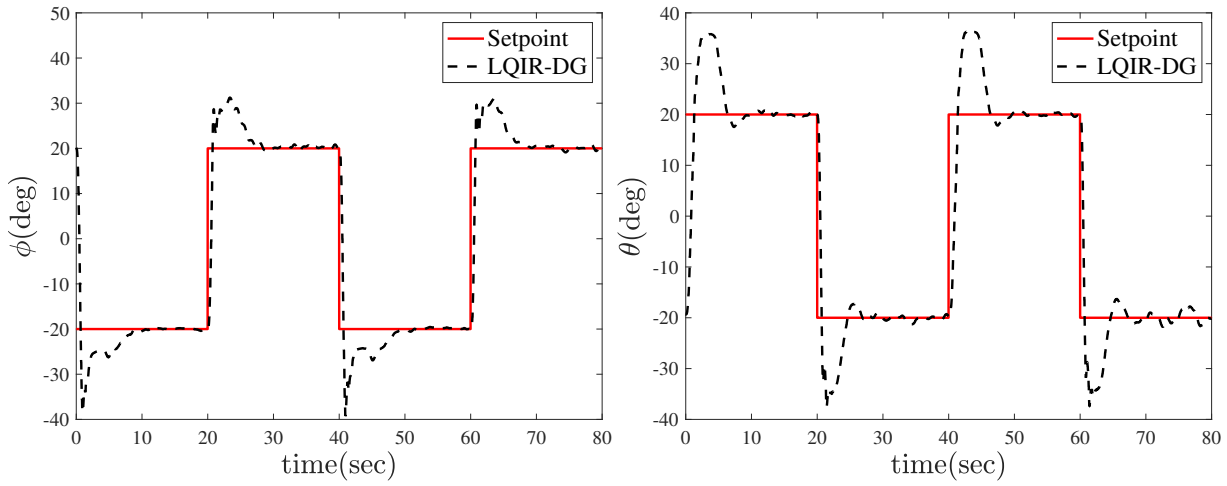

Figure 14: LQIR-DDG controller performance in order to track the desired angles in the two-degree-of-freedom coupling mode (a) Comparison of the roll angle with the desired value (b) Comparison of the pitch angle with the desired

References

[1] M. F. Fathoni, S. Lee, Y. Kim, K.-I. Kim, K. H. Kim, Development of multi-quadrotor simulator based on real-time hypervisor systems, Drones 5 (3). doi:10.3390/drones5030059.
URL https://www.mdpi.com/2504-446X/5/3/59

[2] H. Nobahari, A. Sharifi, A hybridization of extended kalman filter and ant colony optimization for state estimation of nonlinear systems, Applied Soft Computing 74. doi:10.1016/j.asoc.2018.10.010.

[3] H. Bolandi, M. Rezaei, R. Mohsenipour, H. Nemati, S. Smailzadeh, Attitude control of a quadrotor with optimized pid controller, Intelligent Control and Automation 04 (2013) 342–349. doi:10.4236/ica.2013.43040.

[4] A. Abdul Salam, I. Ibraheem, Nonlinear pid controller design for a 6-dof uav quadrotor system, Engineering Science and Technology, an International Journal 22. doi:10.1016/j.jestch.2019.02.005.

[5] Y. Bouzid, M. Zareb, H. Siguerdidjane, M. Guiatni, Boosting a Reference Model-Based Controller Using Active Disturbance Rejection Principle for 3D Trajectory Tracking of Quadrotors: Experimental Validation, Journal of Intelligent and Robotic Systems 100 (2) (2020) 597–614. doi:10.1007/s10846-020-01182-4.
URL https://hal.univ-grenoble-alpes.fr/hal-02543214

[6] Z. Wang, D. Huang, T. Huang, N. Qin, Active disturbance rejection control for a quadrotor uav, in: 2020 IEEE 9th Data Driven Control and Learning Systems Conference (DDCLS), 2020, pp. 1–5. doi:10.1109/DDCLS49620.2020.9275226.

[7] K. Liu, R. Wang, S. Dong, X. Wang, Adaptive fuzzy finite-time attitude controller design for quadrotor uav with external disturbances and uncertain dynamics, in: 2022 8th International Conference on Control, Automation and Robotics (ICCAR), 2022, pp. 363–368. doi:10.1109/ICCAR55106.2022.9782598.

[8] L. V. Nguyen, M. D. Phung, Q. P. Ha, Iterative learning sliding mode control for uav trajectory tracking, Electronics 10 (20). doi:10.3390/electronics10202474.
URL https://www.mdpi.com/2079-9292/10/20/2474

[9] C. Nicol, C. Macnab, A. Ramirez-Serrano, Robust neural network control of a quadrotor helicopter, in: 2008 Canadian Conference on Electrical and Computer Engineering, 2008, pp. 001233–001238. doi:10.1109/CCECE.2008.4564736.

[10] C.-H. Pi, W.-Y. Ye, S. Cheng, Robust quadrotor control through reinforcement learning with disturbance compensation, Applied Sciences 11 (7). doi:10.3390/app11073257.
URL https://www.mdpi.com/2076-3417/11/7/3257

[11] P. Ghiglino, J. L. Forshaw, V. J. Lappas, Online PID Self-Tuning using an Evolutionary Swarm Algorithm with Experimental Quadrotor Flight Results. arXiv:https://arc.aiaa.org/doi/pdf/10.2514/6.2013-5098, doi:10.2514/6.2013-5098.
URL https://arc.aiaa.org/doi/abs/10.2514/6.2013-5098

[12] A. Aboudonia, A. El-Badawy, R. Rashad, Disturbance observer-based feedback linearization control of an unmanned quadrotor helicopter, Proceedings of the Institution of Mechanical Engineers Part I Journal of Systems and Control Engineering 230. doi:10.1177/0959651816656951.

[13] H. Wang, M. Chen, Sliding mode attitude control for a quadrotor micro unmanned aircraft vehicle using disturbance observer, in: Proceedings of 2014 IEEE Chinese Guidance, Navigation and Control Conference, 2014, pp. 568–573. doi:10.1109/CGNCC.2014.7007285.

[14] K. Chara, A. Yassine, F. Srairi, K. Mokhtari, A robust synergetic controller for quadrotor obstacle avoidance using bézier curve versus b-spline trajectory generation, Intelligent Service Robotics 15. doi:10.1007/s11370-021-00408-0.

[15] A. T. Azar, F. E. Serrano, A. Koubaa, N. A. Kamal, Backstepping h-infinity control of unmanned aerial vehicles with time varying dis-

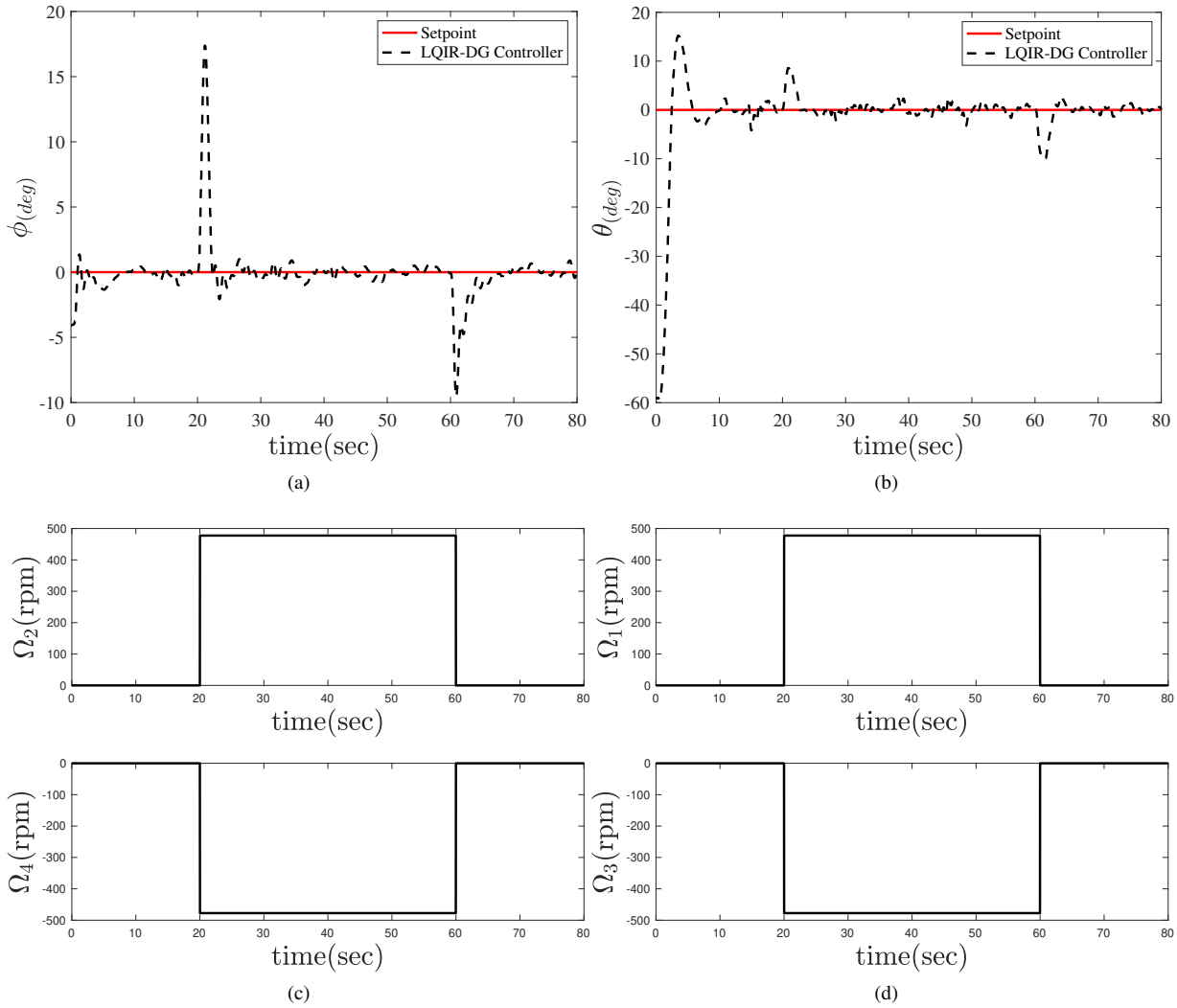

Figure 15: The performance of the LQIR-DG controller in the presence of the input disturbance in the two-degree-of-freedom coupling mode (a) Comparison of the desired roll angle with the actual value (b) Comparison of the desired pitch angle with the actual value.

turbances, in: 2020 First International Conference of Smart Systems and Emerging Technologies (SMARTTECH), 2020, pp. 243–248. doi:10.1109/SMART-TECH49988.2020.00061.

[16] A. Hamza, A. Mohamed, A. El-Badawy, Robust h-infinity control for a quadrotor uav, 2022. doi:10.2514/6.2022-2033.

[17] W. Dean, B. Ranganathan, I. Penskiy, S. Bergbreiter, J. Humbert, Robust Gust Rejection on a Micro-air Vehicle Using Bio-inspired Sensing, 2017, pp. 351–362.

[18] Z. Shulong, A. Honglei, Z. Daibing, S. Lincheng, A new feedback linearization lqr control for attitude of quadrotor, in: 2014 13th International Conference on Control Automation Robotics and Vision (ICARCV), 2014, pp. 1593–1597. doi:10.1109/ICARCV.2014.7064553.

[19] E. Barzanooni, K. Salahshoor, A. Khaki Sedigh, Attitude flight control system design of uav using lqg ltr multivariable control with noise and disturbance, in: 2015 3rd RSI International Conference on Robotics and Mechatronics (ICROM), 2015, pp. 188–193. doi:10.1109/ICRoM.2015.7367782.

[20] J. Engwerda, Linear quadratic games: An overview, Workingpaper, Macroeconomics, subsequently published in Advances in Dynamic Games and their Applications (book), 2009 Pagination: 32 (2006).

[21] J. Engwerda, Min-max robust control in lq-differential games, Dynamic Games and Applications 12 (2022) 1–59. doi:10.1007/s13235-021-00421-z.

[22] Z. Zwierzewicz, On the ship course-keeping control system design by using robust and adaptive control, in: 2014 19th International Conference on Methods and Models in Automation and Robotics (MMAR), 2014, pp. 189–194. doi:10.1109/MMAR.2014.6957349.

[23] Y. Li, L. Guo, Towards a theory of stochastic adaptive differential games, in: 2011 50th IEEE Conference on Decision and Control and

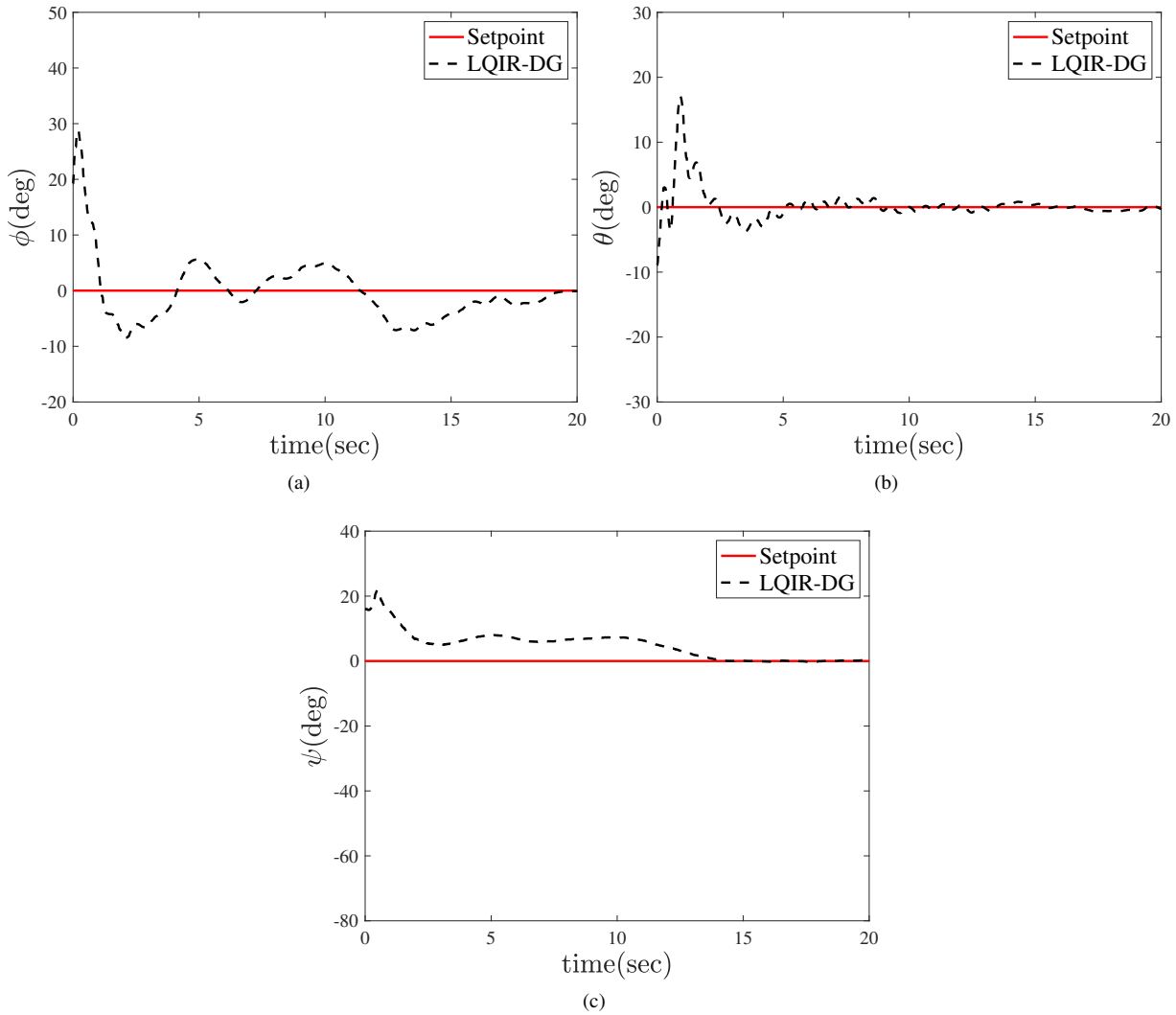

Figure 16: The performance of the LQIR-DG controller by adding weight to each of the roll and pitch axes in the three-degree-of-freedom coupling mode (a) Comparison of the roll angle with the actual value (b) Comparison of the pitch angle with the actual value (c) Comparison of the yaw angle with the actual value

European Control Conference, 2011, pp. 5041–5046. doi:10.1109/CDC.2011.6160768.

[24] K. Zhang, J. Chen, Y. Chang, Y. Shi, Ekf-based lqr tracking control of a quadrotor helicopter subject to uncertainties, in: IECON 2016 - 42nd Annual Conference of the IEEE Industrial Electronics Society, 2016, pp. 5426–5431. doi:10.1109/IECON.2016.7794149.

[25] S. I. Azid, K. Kumar, M. Cirrincione, A. Fagiolini, Robust motion control of nonlinear quadrotor model with wind disturbance observer, IEEE Access 9 (2021) 149164–149175. doi:10.1109/ACCESS.2021.3124609.

[26] S. Bouabdallah, R. Siegwart, Full control of a quadrotor, in: 2007 IEEE/RSJ International Conference on Intelligent Robots and Systems, 2007, pp. 153–158. doi:10.1109/IROS.2007.4399042.

[27] S. Bouabdallah, Design and control of quadrotors with application to autonomous flyingdoi:10.5075/epfl-thesis-3727.

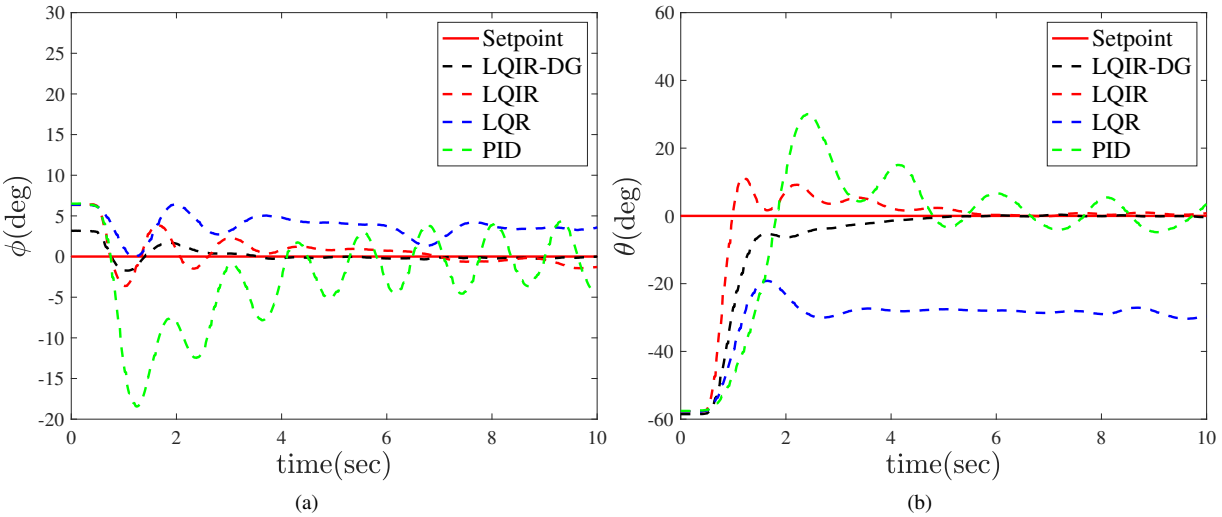

Figure 17: The performance of the LQIR-DG controller by adding weight to each of the roll and pitch axes in the three-degree-of-freedom coupling mode (a) Comparison of the roll angle with the actual value (b) Comparison of the pitch angle with the actual value (c) Comparison of the yaw angle with the actual value

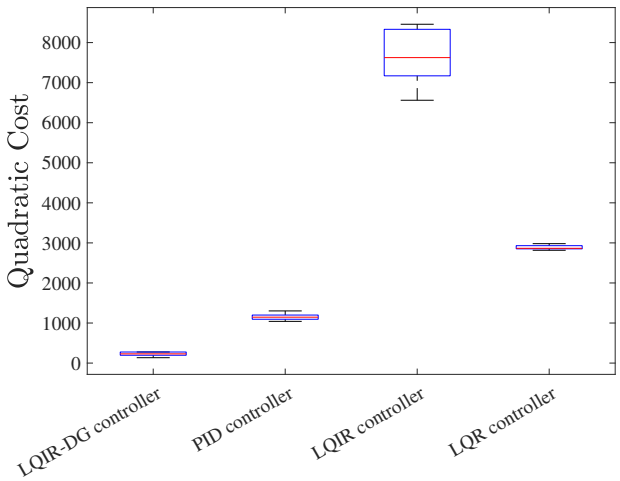

Figure 18: Comparison of the LQIR-DG to the PID quadratic cost function